FLEXURAL BEHAVIOR OF A FULL-SCALE SELF-CONSOLIDATING CONCRETE PRESTRESSED GIRDER

Young Hoon Kim, Texas A&M University, College Station, TX
David Trejo, PhD, PE, Texas A&M University, College Station, TX
Mary Beth D. Hueste, PhD, PE, Texas A&M University, College Station, TX

ABSTRACT

To achieve adequate flow and homogeneous concrete for precast, prestressed members, self-consolidating concrete (SCC) typically has to have higher paste and lower coarse aggregate volume than conventional concrete (CC). Because the coarse aggregate content and paste volume can potentially affect the hardened properties, SCC may not provide the same in-service performance as CC. This research program investigated the flexural capacity and bond properties of a SCC prestressed bridge girder and compared these results with those obtained from a similar CC specimen. The concrete mixtures had a target 16-hour release strength of 5000 psi (35 MPa). A deck was cast on the girders and prestress losses were monitored prior to destructive testing of the composite girder-deck system. This testing was performed to evaluate the flexural capacity of the system. These results were also used to evaluate the applicability of the current American Association of State Highway and Transportation Officials Load and Resistance Factor Design (AASHTO LRFD) Specifications for the design of precast, prestressed, SCC bridge girders. Test results indicate that the flexural capacity and bond performance of the SCC girder are similar to those of the CC girder.

Keywords: Self-Consolidating Concrete, Prestressed Concrete Bridge, Flexural Capacity, Prestress Loss, Transfer Length, Development Length, Camber and Deflection, AASHTO Specifications

INTRODUCTION

According to ACI Committee 237, self-consolidating concrete (SCC) is defined as a "highly flowable, nonsegregating concrete that can spread into place, fill the formwork, and encapsulate the reinforcement without any mechanical consolidation[1]." To achieve key fresh characteristics, such as high workability and stability, SCC typically has higher paste and lower coarse aggregate volumes than conventional concrete (CC)[2]. Optimized dosages of chemical admixtures [high-range water reducing admixtures (HRWRAs)] can provide both resistance to segregation and high workability. Several researchers have characterized SCC mixture proportions and provided guidelines[3, 4]. However, hardened properties of high early strength SCC have been studied only on a limited basis and reliable data are needed for precasters who are eager to use SCC. The use of SCC in precast, prestressed concrete products is an especially demanding application of this technology. However, there are a number of potential benefits, including: a) better finish quality of completed products, b) less noise on job sites, c) decreased time for placement, d) lower maintenance cost of construction equipment, e) lower labor demands, and f) better quality concrete[5]. Because the coarse aggregate content and paste volume can potentially affect the hardened properties, SCC may not provide the same in-service performance as CC. This research investigated the transfer and development lengths, prestress losses, and flexural behavior of a SCC prestressed bridge girder and compared these results with those obtained for a similar CC specimen.

EXPERIMENTAL PROGRAM

TxDOT Type A girders were designed in accordance with the AASHTO LRFD Bridge Design Specifications (2006)[6] and the TxDOT Bridge Design Manual[7]. One CC girder and one SCC girder were fabricated at a precast plant.

River gravel coarse aggregate was used for the SCC and CC (control) girders. The dimensions of the Type A girder cross section are shown in Fig. 1. The 40 ft (12.2 m) long CC and SCC girders were fabricated with the same prestressing conditions and were monitored continuously. The losses of the prestressing strands were measured at the time of release and at later ages. In addition, the mechanical properties were evaluated. After approximately seven weeks, concrete decks [64 in. wide (1.63 m) and 8 in. thick (0.2 m)] were cast on the girders.

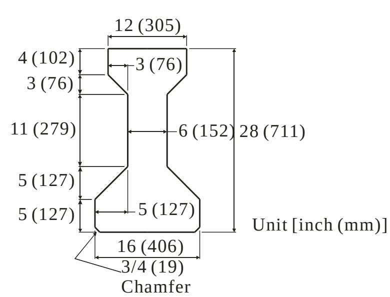

Fig. 1. Cross Section and Dimensions of Type A Girder

EXPERIMENTAL PLAN

The CC and SCC girders were fabricated at a precast plant in Texas, transported from the prestressing bed to a storage area, and then transported to the High Bay Structural and Materials Laboratory (HBSML) at Texas A&M University. Fabrication of the decks was performed in the HBSML. Concrete strains and temperature were monitored continuously at the plant and HBSML.

MATERIALS

Girders

Three SCC mixture proportions with river gravel were evaluated with the main variable being the volume of the coarse aggregate (ranging from 29-38 percent). The coarse aggregate is natural river gravel with a rounded shape. The gradation of the coarse aggregate met the requirement of ASTM C33, *Standard Specification for Concrete Aggregates*[8]. The target release strength was 5000 psi (35 MPa)[9, 10]. Among the three SCC mixture proportions considered in this research program, the mixture proportion with the highest volume of river gravel aggregate was used in the SCC Type A girder. Mixture proportions are presented in Table 1.

Table 1 Mixture Proportions

Girder I.D.	CC-R	SCC-R
Targeted 16-hr (release) strength	5000 psi (34 MPa)	5000 psi (34 MPa)
Aggregate Type	River gravel	River gravel
Cement, lb/yd^3 (kg/m^3)	625 (371)	633 (376)
Fly Ash, lb/yd^3 (kg/m^3)	0	298 (177)
Water, lb/yd^3 (kg/m^3)	225 (134)	255 (152)
Coarse Aggregate, lb/yd^3 (kg/m^3)	1935 (1148)	1649 (978)
Fine Aggregate, lb/yd^3 (kg/m^3)	1232 (731)	1095 (650)
HRWR (Type I), oz/yd^3 (L/m^3)	56 (2.2)	-
HRWR (Type II), oz/yd^3 (L/m^3)	-	82 (3.2)
Retarder, oz/yd^3 (L/m^3)	0	25 (1)

Two girders, one with CC and one with SCC (CC-R and SCC-R), were fabricated on March 26, 2007. A Type III cement (Alamo Cement Company, San Antonio, Texas), the same silo used in the laboratory testing phase of the research program, was used for the full-scale testing. Untreated Class F fly ash (Boral Material Technologies, Rockdale, Texas) was used for supplementary cementitious materials (SCM). Admixtures were provided by BASF Construction Chemicals LLC. Because release strength is critical for plant productivity, precast industries use high early strength concrete. Both the CC and SCC mixture proportions were designed to achieve a target compressive strength of 5000 psi (34 MPa) at 16 hours. High workability and stability were also required of the SCC mixture. In this study, fly ash was used in the SCC mixture to increase the paste content and achieve high workability and high early strength. In typical CC mixtures in Texas, the use of cement is typically sufficient to achieve the necessary workability and high early strength.

The cement, water, and aggregate were initially batched and mixed, followed by adding and mixing in the retarder and finally adding a HRWRA into the mixture. After sufficient mixing, the concrete was discharged into a bucket auger with an approximate drop height from the mixer to the bucket auger of 3 to 5 ft (0.9 m to 1.5 m). For the CC, the concrete was continuously discharged into the forms while moving along the forms. Mechanical vibration was used to consolidate the CC. For the SCC mixture, the majority of the concrete was placed in the form from one end. As the form was filled, the forklift with the bucket auger was moved along the form to complete the placement. No consolidation was used for the girders containing SCC. For the fresh properties, the slump flow, T_{50}, and visual stability index (VSI) of the SCC mixtures were measured and recorded. The slump flow is the measured maximum diameter of flow after lifting the inverted slump cone. The T_{50} value represents the time in seconds when a flow patty reaches a diameter of 20 in. (50 cm). The VSI is a visual examination to rank the stability of the SCC on a scale of 0 to 3 in 0.5 increments. A VSI of 0 is highly stable and represents an ideal condition, while a VSI of 3 is highly unstable resulting in rejection of an SCC mixture. Small samples were cast from the same batches used for the girders to evaluate the mechanical properties of the precast concrete. The concrete for the deck was also tested and characterized. Embedded strain gages were used to evaluate the loss of the prestressing strands in the girder.

Grade 60 reinforcement meeting ASTM A615, *Standard Specification for Deformed and Plain Carbon-Steel Bars for Concrete Reinforcement*, was used for the girders. The actual yield strength, f_y , of the mild reinforcement was 69 ksi (476 MPa). The prestressing steel for the girders was 0.5 in. diameter, Grade 270, low-relaxation, seven-wire strand manufactured by American Spring Wire Corporation in Houston, Texas. The strand met the requirement of ASTM A416, *Standard Specification for Steel Strand, Uncoated Seven-Wire for Prestressed Concrete*.

The Type A girder was designed in accordance with the AASHTO LRFD Bridge Design Specifications (2006) and the TxDOT Bridge Design Manual (2001). Ten straight strands were used in the bottom flange to control the bottom fiber stress at midspan. Two straight tendons were placed in the top flange to control the top fiber stress at the girder ends. The mild steel reinforcement was placed in accordance with the AASHTO LRFD Bridge Design Specifications (2006) and the TxDOT Bridge Design Manual (2001).

Decks

In accordance with TxDOT Design Manual, TxDOT Class S concrete was used for the cast-in-place (CIP) decks. This concrete was provided by a local ready mix concrete plant. Class

S concrete is normally proportioned for a minimum compressive strength of 4000 psi (28 MPa) at 28 days. The deck was 8 in. (200 mm) thick and 64 in. (1600 mm) wide.

Grade 60 reinforcement meeting ASTM A615 was used for the CIP decks, with actual yield strength, f_y, of 62 ksi (427 MPa). Longitudinal and lateral reinforcement was placed in the deck to mimic actual deck construction practices in Texas. Two layers of #5 US (M16) and #4 US (M13) mild reinforcement were used with 7 to 9 in. (180 to 230 mm) spacing to control shrinkage and temperature.

TRANSFER LENGTH

Instrumented locations for the embedded concrete strain gages are shown in Fig. 2. Both ends of the beam have the same instrumentation set-up. These gages were used to measure transfer length and prestress losses. Transfer length is defined as the transition distance from the free end of the strands to the fully bonded zone having the effective stress of the strands. The value of the transfer length was determined by the 95 percent Maximum Average Strain (MAS) method[11]. According to the AASHTO LRFD Specifications (2006), the transfer length is estimated as 60 times the strand diameter.

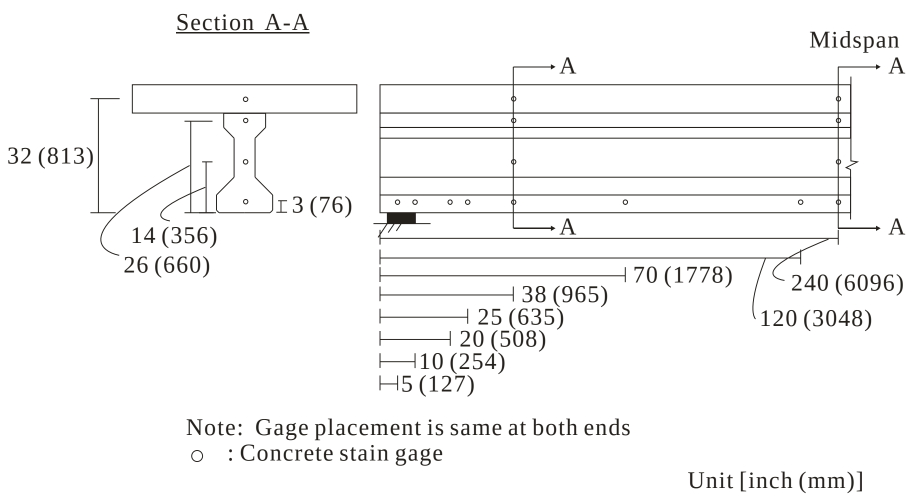

Fig. 2. Strain Gage Locations

CAMBER AND DEFLECTION

Camber and deflection were measured with string potentiometers and strain gages at midspan (shown in Fig. 2). When the deflection stabilized, the deflection monitoring was terminated.

PRESTRESS LOSSES

Initial Strand Stresses

Load cells were used to measure the jacking stresses, f_{pj}, and the initial stress at release, f_{pi}, for each girder. The load cells compensated for induced moments, torsional moments, and temperature effects.

Elastic Shortening and Long-Term Prestress Losses

Elastic shortening, elastic gain, and long-term losses due to combined creep and shrinkage of the girder and deck were measured using the embedded concrete strain gages.

FLEXURAL TESTS

Flexural Capacity

After monitoring strain profiles for approximately 18 weeks after casting, the girders were evaluated for flexural behavior and capacity at the HBSML. A hydraulic ram with a 600 kip (2700 kN) capacity was used to apply a load at the beam center with a spreader beam having load points spaced at 36 in. (910 mm) centers. The data acquisition system recorded data every 5 seconds. Strain gages and linear variable differential transducers (LVDTs) were monitored to investigate bond between the strands and concrete, moment-curvature, load-displacement, and cracking. When the moment capacity of the composite girder reached the nominal value, indicated by 3000 microstrain at the top concrete surface, testing was terminated. Fig. 3 shows the flexural test set-up.

Fig. 3. Overview of Flexural Test Set-up

Bond Performance after Cracking

To monitor the bond of the strands at the beam ends, strain gages were attached to the bottom flange of the girder and were located at the same level as the centroid of the strands, as shown in Fig. 4. Concrete strain gages were also used to detect failure of strands and concrete cracks.

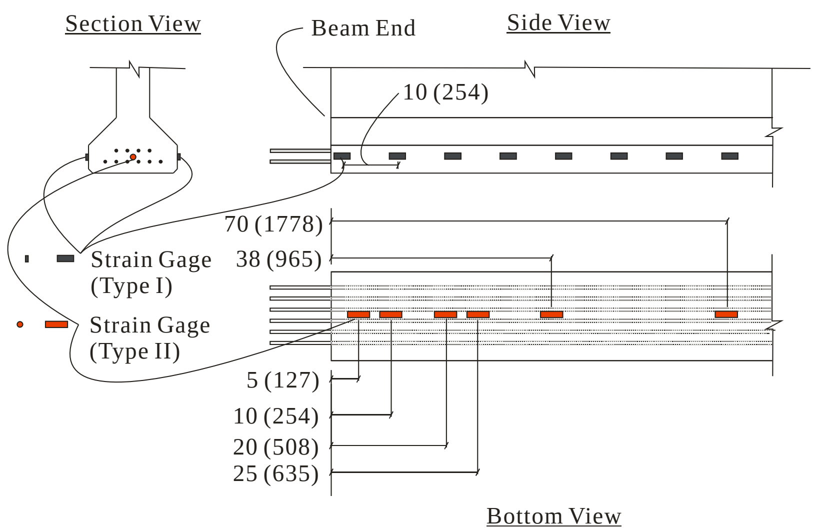

Fig. 4. Diagram of Concrete Surface Strain Gage Layout (Type I)
and Embedded Concrete Strain Gage Layout (Type II)

Bond Performance (Constant Moment Region)

LVDTs were installed to investigate the strain profile and crack width within the constant moment region. Fig. 5 shows the LVDT installation locations used to measure the strain of strands in the bottom flange.

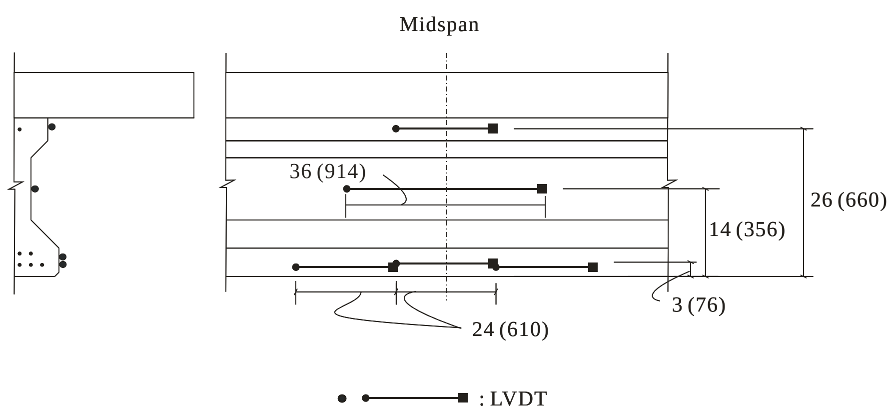

Fig. 5. Average Strain of Strains of Constant Moment Region

Cracks at Midspan

Crack patterns and maximum crack widths with 0.002 in. (0.05 mm) accuracy were manually recorded after each loading step.

DEVELOPMENT LENGTH TESTS

The embedment length, l_e, is the length of the embedded strands from the girder end to the loading point for the development length test. Transfer length, l_t, is defined as the transition distance from the free end of the strands to the fully bonded zone having the effective stress of the strands at service, f_{pe}. Flexural bond length, l_f, is the additional bond length added to the transfer length for the strands to reach the stress, f_{ps}, corresponding to the nominal moment capacity of the girder. The development length, l_d, is estimated to be the sum of l_t and l_f. If the test reaches nominal flexural conditions, then the theoretical value of l_d is either equal to or less than the value of l_e. To determine the transition point from a flexural to a bond failure, l_e can be varied from test to test. Embedment lengths longer than the required l_d will result in a flexural failure. Embedment lengths shorter than l_d should result in a bond/shear failure or bond/flexural failure. To confirm flexural failure, the strain on the top concrete surface is required to reach or exceed 3000 microstrain. Bond failure can be observed by slip of the strands and a sudden loss of capacity such as a shear failure. Two development length tests were conducted for each girder, one at each girder end. According to the AASHTO LRFD Specifications (2006), the strand development length l_d for design can be determined as follows:

$$l_d \geq \kappa\left(f_{ps} - \frac{2}{3} f_{pe}\right) d_b \quad \left[l_d \geq \frac{\kappa}{6.9}\left(f_{ps} - \frac{2}{3} f_{pe}\right) d_b\right] \tag{1}$$

where d_b is the nominal strand diameter [in. (mm)], f_{ps} is the average stress in the prestressing steel at the time for which the nominal resistance of the member is required [ksi (MPa)], f_{pe} is the effective stress in the prestressing steel after losses [ksi (MPa)], and κ is 1.0 for pretensioned panels, piling, and other pretensioned members with a depth of less than or equal to 24 in. (610 mm) or 1.6 for pretensioned members with a depth greater than 24 in. (610 mm).

CC-R1 and CC-R2 Tests

After completing the flexural tests, each end of the composite girder was tested to determine the development length. The CC-R girder development length tests consisted of one test at each girder end, denoted as CC-R1 and CC-R2. The interior support was located at 162 in. (4.1 m) from the girder end, as shown in Fig. 6. The loading increments and measured parameters were the same as those used for the midspan flexural tests.

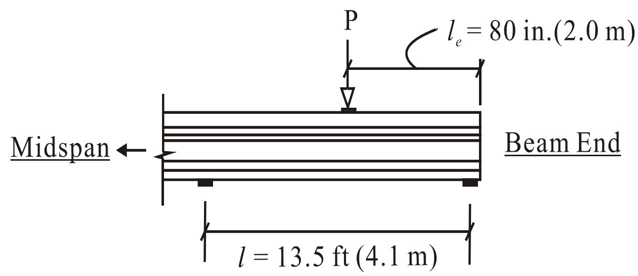

Fig. 6. Test Set-up for Development Length Test CC-R1

After testing the CC-R1 end, the CC-R2 end test was performed with a 150 in. (3.8 m) span length and a reduced l_e of 70 in. (1.8 m), as shown in Fig. 7. It should be noted that the end span included some flexural cracks from the flexural testing near the interior supports.

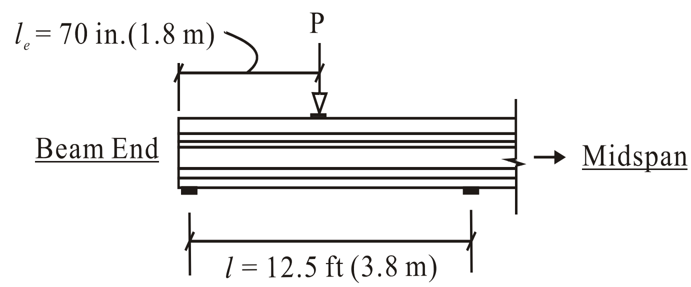

Fig. 7. Test Set-up for Development Length Test CC-R2

SCC-R1 and SCC-R2 Tests

Development length tests for the SCC-R girder were also conducted at each girder end. The span and embedment lengths were 162 in. (4.1 m) and 80 in. (2.0 m), respectively. For SCC-R2, the overhead crane was used to support the girder weight at the free end, as shown in Fig. 8.

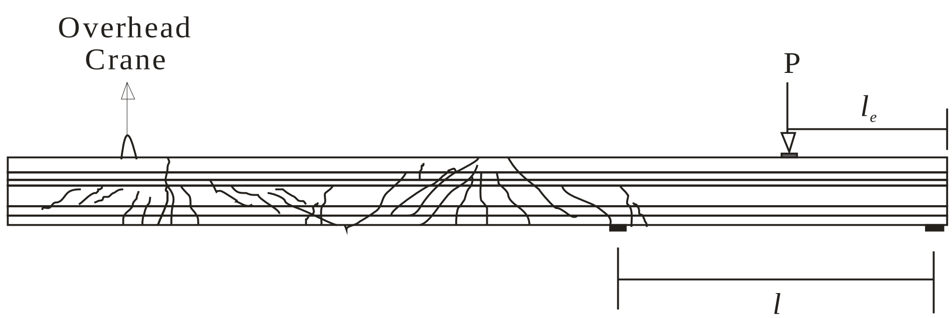

Fig. 8. Modified Development Length Test for SCC-R2

TEST RESULTS

Material properties, mechanical properties, prestress loss and flexural test results are presented in the following sections.

MATERIALS

Girders

Each girder required concrete from two batches. The fresh characteristics were evaluated in the field and are presented in Table 2. All SCC mixtures had proper fresh characteristics with high workability and vibration was not used, resulting in a significant reduction in noise, labor, and casting time.

Table 2. Measured Fresh Properties and Compressive Strength

Girder I.D.	CC-R		SCC-R	
Batch Number	1	2	1	2
Ambient Temp. ,°F	72			
Slump, in.	8	-	-	-
Slump Flow, in.	-	-	27.0	28.5
T_{50}, s	-	-	3.3	3.6
VSI	-	-	1.0	1.5

Table 3 shows the measured material properties of the concrete for the decks and girders corresponding to the date of flexural testing. The strand stresses after losses f_{pe} measured on the structural test date are also provided.

Table 3. Measured Properties of Materials

Material	Property	CC-R	SCC-R
Girder Concrete	Average f_c', psi (MPa)	9620 (66.4)	12,840 (88.5)
	Std. Dev. f_c', psi (MPa)	251 (1.73)	256 (1.77)
CIP Deck Concrete	Average f_c', psi (MPa)	6170 (42.5)	7530 (51.9)
	Std. Dev. f_c', psi (MPa)	227 (1.57)	143 (0.99)
Prestressing Strands	f_{pe}, ksi (MPa)	201 (1.39)	200 (1.38)

The development of compressive strength was evaluated with three 4 x 8 in. (100 x 200 mm) cylinders at 16 hours, at release, and at 3, 7, 28, and 91 days. The release strengths of the CC and SCC met the 5000 psi (35 MPa) target strength requirements. As shown in Table 4, the SCC mixture exhibited about 30 percent higher compressive strength than the CC mixture at 91 days.

Table 4. Development of Compressive Strength

Girder I.D.	CC-R	SCC-R
16 hr Strength, psi (MPa)	5080 (35)	5714 (39)
Release, psi (MPa)	6360 (44)	6510 (45)
3 days, psi (MPa)	7285 (50)	7499 (52)
7 days, psi (MPa)	7765 (54)	8807 (61)
28 days, psi (MPa)	8982 (62)	11,151 (77)
91 days, psi(MPa)	9440 (65)	12,055 (83)

Decks

The deck concrete of the SCC-R girder exhibited a 22 percent higher 28-day compressive strength when compared with the deck concrete of the CC-R girder, as shown in Table 5.

Table 5. 28-day Compressive Strength of CIP Deck Concrete

Parameter	CC-R	SCC-R
Average f_c', psi (MPa)	6480 (45)	7920 (54)
Std. Dev. f_c', psi (MPa)	395 (2.7)	177 (1.2)

TRANSFER LENGTH

The transfer length for each end of the girders was determined. The initial transfer length, l_{tri}, was measured immediately after release. The final transfer length, l_{trf}, was measured when the monitoring was terminated prior to structural testing of the girder. Fig. 9 shows that the initial and final (140 days) transfer lengths of both girders were shorter than $60d_b$, the value specified by the AASHTO LRFD Specifications (2006). Each error bar in the graphs indicates the maximum and minimum transfer lengths for the corresponding girder. The CC girder has an approximately 50 percent higher average measured transfer length than the SCC girder for the initial and final transfer length measurements. The final transfer length was approximately two times the initial transfer length for both girders.

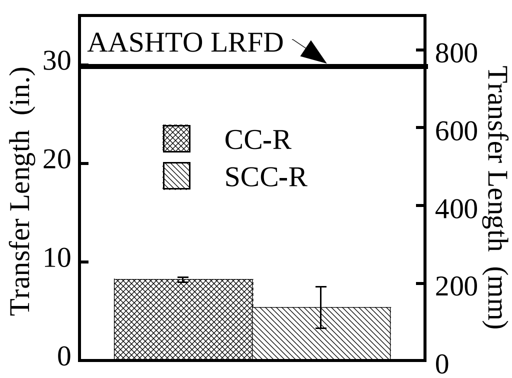

(a) Initial Transfer Length, l_{tr}

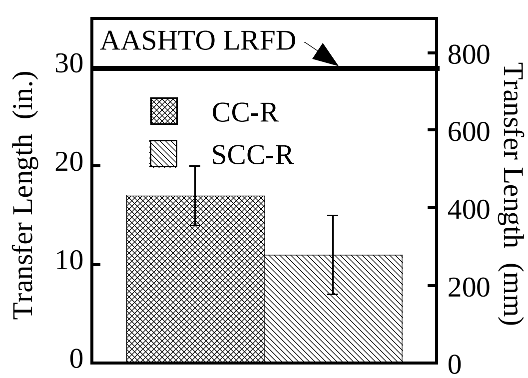

(b) Final Transfer Length, l_{tf}

Fig. 9. Initial and Final (140 days) Transfer Length Measurements

CAMBER AND DEFLECTION

Fig. 10 shows the history of camber and deflection of the prestressed girders and the composite girder and deck systems. The deflection of both girders was measured with string pots and strain gages in the field and in the HBSML for about 130 days. The initial camber growth of the CC girder was higher than that of the SCC girder. The final deflection values of the CC and SCC girders were within 0.25 in. (6 mm) at 130 days, indicating that long-term deflection is similar for both girders. The increased paste content of the SCC mixture suggests that the creep and deflection would be higher for SCC mixtures. However, the higher later age compressive strength likely compensated for this.

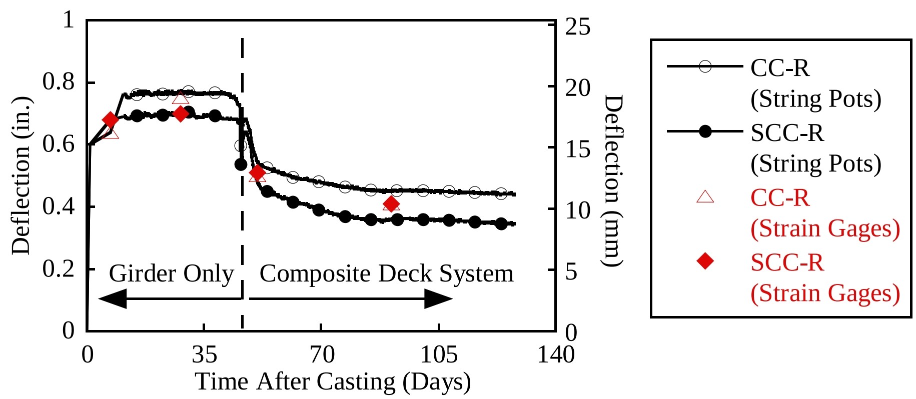

Fig. 10. History of Camber and Deflection for Girder and Composite Girder-Deck Systems

PRESTRESS LOSSES

Initial Stresses of Strands

The strand jacking stresses and strand stresses immediately before transfer were monitored with load cells. Both girders were tensioned in the same prestressing bed. Significant loss of anchorage seating was not observed at tensioning. Strand stresses between the time of casting and the time of transfer were continuously monitored at five second intervals. In the design equation from the AASHTO LRFD Specifications (2006), the relaxation of strands can be estimated after tensioning of strands. The stresses on the strands are time-dependent values due to relaxation of strands as follows:

$$f_{pbt} = f_{pj} - \Delta f_{pR}(t_0, t_{tr}) \tag{2}$$

where f_{pbt} is the strand stress immediately before transfer [ksi (MPa)], f_{pj} is the initial jacking stress [ksi (MPa)], t_0 is the time at jacking (hr), t_{tr} is the time at transfer (hr), and $\Delta f_{pR}(t_0, t_{tr})$ is the relaxation of strands between t_0 and t_{tr} [ksi (MPa)]. There were no apparent prestress losses due to relaxation before transfer. The average stresses of strands in the bottom layers at each event are summarized in Table 6, along with the corresponding standard deviation. Because girders CC-R and SCC-R were fabricated at the same time, the values apply to both girders.

Table 6. Strand Stresses in Bottom Layers (CC-R and SCC-R)

Description	Time	Avg.	Std. Dev.
Initial Jacking Stress, f_{pj} at t_0, ksi (MPa)	3/22/07 4:30 PM	208.5 (1438)	3.93 (27)
Stress at Casting, f_{pj}, ksi (MPa)	3/26/07 4:42 PM	212.4 (1464)	4.57 (32)
Stress Immediately Before Transfer, f_{pbt}, ksi (MPa)	3/27/07 3:20 PM	213.0 (1469)	4.72 (33)

Elastic Shortening and Long-Term Prestress Losses

The strain readings immediately before transfer were taken as the base values. To estimate the elastic shortening, the elastic modulus of the concrete at transfer is estimated based on the strength of concrete at transfer. Thermal changes of the strands were not significant prior to and after transfer and did not result in a change in the strand stress.

Table 7 shows the estimated prestress losses due to elastic shortening at the midspan of the girders. The SCC-R girder had approximately 7 percent higher losses due to elastic shortening than the CC-R girder, corresponding to a relatively small difference in the elastic shortening loss of approximately 0.5 ksi (3 MPa).

Table 7. Elastic Shortening at Transfer Measured at Midspan

Girder I.D.	$\Delta\varepsilon_{pES}$, x10^{-6} in./in. (x10^{-6} mm/mm)	Concrete Temperature, ^oF (^oC) *	$\Delta\varepsilon_t$, ksi (MPa)	Δf_{ES}, ksi (MPa)
CC-R	236 (236)	85 (29)	0	6.61 (46)
SCC-R	253 (253)	85 (29)	0	7.09 (49)

Notes: *Ambient temperature

$\Delta\varepsilon_{pES}$ is the measured girder strain caused by elastic shortening, $\Delta\varepsilon_t$ is the thermal strain at transfer, and Δf_{ES} is the prestress loss caused by elastic shortening

Long-term prestress losses prior to deck placement mainly occurred from concrete shrinkage, along with creep due to sustained loading from the axial prestressing force and girder self-weight. After casting the deck, the composite girder and deck system experienced prestress losses from creep with the sustained load stress increasing due to the deck weight, and from shrinkage of the girder and deck. The relaxation of the strands also contributed to the long-term prestress losses. As shown in Table 8, the overall comparison shows that CC-R had lower total elastic shortening and long-term losses when compared with the SCC-R girder. The SCC-R mixture had a higher paste volume and a lower aggregate volume resulting in a lower stiffness and higher deformation under the same axial prestressing force.

The AASHTO LRFD Specifications (2006) provide equations to estimate the prestress losses by considering construction sequence and the creep and shrinkage of the composite girder and deck system. Table 8 shows measured prestress losses at the midspan and the predicted prestress losses according to the AASHTO LRFD Specifications (2006). Positive values indicate prestress losses and negative values indicate prestress gains. The AASHTO time dependent losses were computed to correspond to the age of the girders (approximately 140 days). The SCC and CC girders had similar prestress losses. The AASHTO LRFD expressions overestimated the long-term prestress losses for both the SCC and CC girders. However, it should be noted that the girders were tested at a relatively short time after casting, while long-term loss estimates are typically considered over a much longer period corresponding to the design life of the structure.

Table 8. Summary of Measured and AASHTO Predicted Prestress Losses at Girder Midspan

	Girder I.D.	Elastic Losses, ksi (MPa)	Elastic Gain due to Deck, ksi (MPa)	Long-Term Losses before Deck, ksi (MPa)	Long-Term Losses after Deck, ksi (MPa)	Total Long-Term Losses, ksi (MPa)	Total Prestress Losses, ksi (MPa)
Measured Losses	CC-R	6.61 (46)	-1.05 (-7.2)	5.94 (41)	-1.00 (-6.9)	4.94 (34)	11.5 (80)
	SCC-R	7.09 (49)	-1.12 (-7.7)	7.26 (50)	-1.80 (-12.4)	5.46 (38)	12.6 (87)
AASHTO Losses	CC-R	9.22 (64)	-1.34 (-9.2)	18.6 (128)	13.2 (90.8)	31.8 (219)	39.7 (274)
	SCC-R	9.09 (63)	-1.36 (-9.4)	18.3 (126)	13.0 (89.5)	31.3 (216)	39.1 (269)

FLEXURAL TESTS

Flexural Capacity

Table 9 summarizes the flexural test results. The CC and SCC girders have similar measured nominal moment capacities when the load was applied at midspan. The measured cracking moments of CC-R and SCC-R are within 5 percent of each other. The initial cracking moment for the CC-R girder corresponds to a bottom fiber tensile stress of $13\sqrt{f_c'}$ psi ($1.08\sqrt{f_c'}$ MPa), which is 11 percent higher than the upper bound modulus of rupture [$11.7\sqrt{f_c'}$ psi ($0.97\sqrt{f_c'}$ MPa)] specified by the AASHTO LRFD Specifications (2006). The SCC-R girder exhibited a cracking moment corresponding to a bottom fiber tensile stress of $10.6\sqrt{f_c'}$ psi ($0.88\sqrt{f_c'}$ MPa) which falls within the upper and lower bounds for the modulus of rupture [$11.7\sqrt{f_c'}$ and $7.6\sqrt{f_c'}$ psi ($0.97\sqrt{f_c'}$ and $0.63\sqrt{f_c'}$ MPa)] specified by the AASHTO LRFD Specifications (2006).

Table 9. Summary of Flexural Test Results

Girder I.D.	CC-R	SCC-R
Nominal Moment, kip-ft (kN-m)	1239 (1680)	1258 (1706)
Predicted Nominal Moment, kip-ft (kN-m)	1129 (1531)	1135 (1539)
Cracking Moment, kip-ft (kN-m)	750 (1017)	720 (976)
Predicted Cracking Moment, kip-ft (kN-m)	635 (861)	667 (904)
Coefficient, α of Cracking ($\alpha\sqrt{f_c'}$), psi (MPa)	13.0 (1.08)	10.6 (0.88)
Max. Displacement at Nominal Moment, in. (mm)	5.59 (142)	5.72 (145)

The CC and SCC girders have similar moment-curvature responses. Fig. 11 shows the measured and predicted moment-curvature for the girders. The measured properties of the concrete and strands, along with the measured effective stress of strands after losses, were used to predict the moment-curvature relationship. The predicted relationship was found using the Response 2000 program, which is a sectional analysis tool implementing the Modified Compression Field Theory[12]. As shown by the figure, the overall moment curvature relationship was well predicted using this sectional analysis procedure.

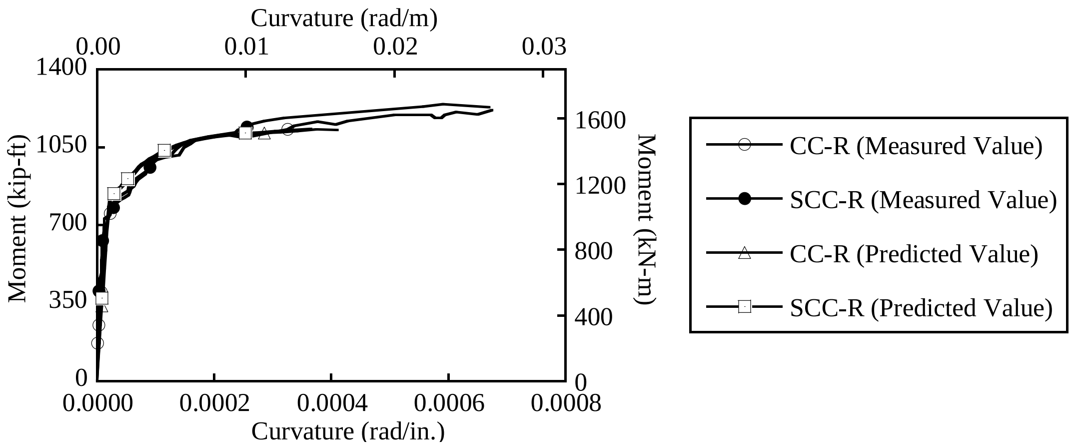

Fig. 11. Moment Versus Curvature Relationship (Measured versus Predicted)

Fig. 12 provides a plot of the applied moment versus the measured crack width at the bottom fiber for each girder. As shown, the crack width in the bottom fiber abruptly changes indicating the moment at cracking.

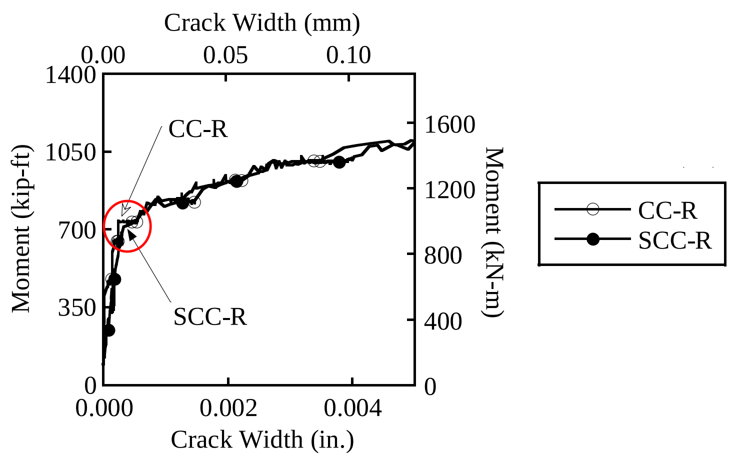

Fig. 12. Cracking Occurrence at the Bottom Girder Fiber

At the nominal flexural condition, the overall behavior at the girders was governed by the capacity of the concrete deck. The strains at the top fiber in the constant moment region for both composite girder and deck systems reached the nominal flexural state, in excess of 3000 microstrain, at the top fiber. Fig. 13 shows the load-deflection curves for the girders loaded at midspan. The girders exhibited almost identical load versus deflection responses.

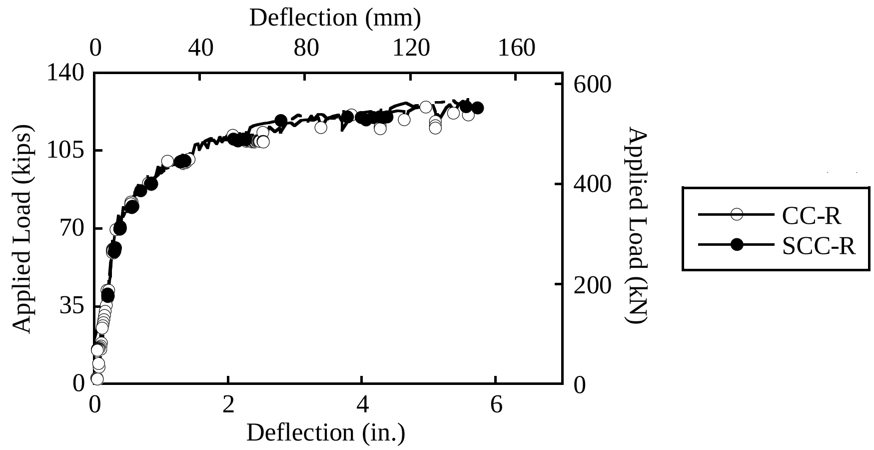

Fig. 13. Deflection of the CC-R and SCC-R Girders

Bond Performance after Cracking (Transfer Length Region)

The overall post-cracking behavior is very similar for the CC and SCC girder and deck systems. Fig. 14 shows the distribution of strain at both ends of each girder at nominal conditions. There was no evidence of bond failure or slip of strands. When the CC and SCC girders were subjected to flexural loading, the bond performance in the transfer region of the both girders exhibited similar behavior after cracking.

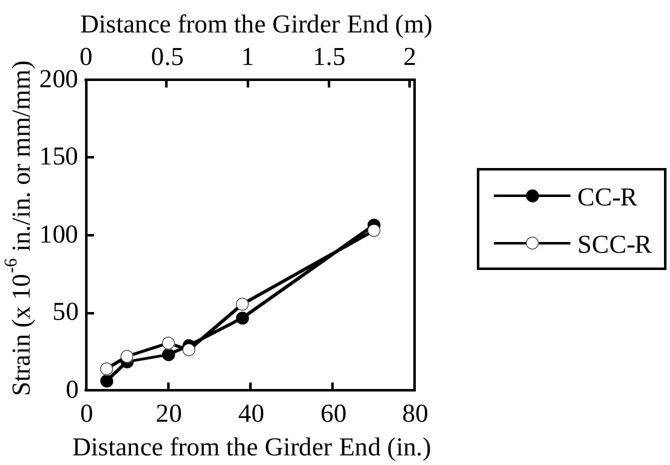

Fig. 14. Distribution of Average Strain at Both Girder Ends

Bond Performance (Constant Moment Region)

As shown in Fig. 15, the overall change of strain in strands subjected to flexural loading was similar for the CC-R and SCC-R girder systems. When the top fiber of the deck exceeded 3000 microstrain, the corresponding average strain of the strands was determined to be approximately 0.02 in./in. (mm/mm).

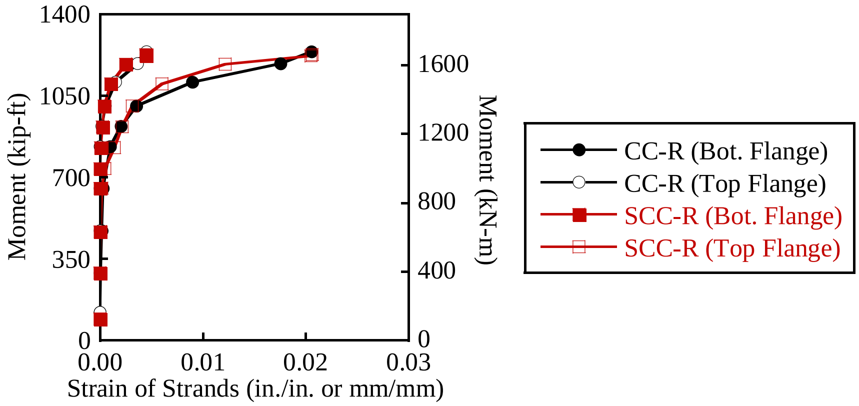

Fig. 15. Average Strain of Strands in Top and Bottom Flanges

Cracks at Midspan

The final crack diagrams for both flexural tests are shown in Fig. 16. Only the cracked regions are shown. In general, the SCC girder exhibited more cracks when compared to the CC girder. The loads corresponding to cracking in the bottom flange, extension of cracking into the top flange, extension of cracking into the deck, and nominal moment are summarized in Table 10, along with the corresponding maximum crack width measurements. The maximum crack width was measured at the extreme tension fiber of the bottom flange. Generally, the progress of flexural cracks and maximum crack widths are similar for both girders. As expected, the flexural cracks propagated into the deck at nominal conditions.

Table 10. Cracking Loads and Maximum Crack Widths

Girder	First Cracking in Bottom Flange		Flexural Cracking into Top Flange		Flexural Cracking into Deck		Nominal Moment	
	Load, kips (kN)	w_{max}, in.(mm)	Load, kips (kN)	w_{max}, in.(mm)	Load, kips (kN)	w_{max}, in.(mm)	Load, kips (kN)	w_{max}, in.(mm)
CC-R	60-80 (270-360)	0.01 (0.3)	100 (445)	0.02 (0.6)	110 (490)	0.05 (1.25)	127 (565)	0.05 (1.25)
SCC-R	70 (311)	0.004 (0.1)	100 (445)	0.01 (0.3)	110 (489)	0.04 (1.0)	126 (560)	0.06 (1.5)

Note: w_{max} = Maximum crack width in bottom flange

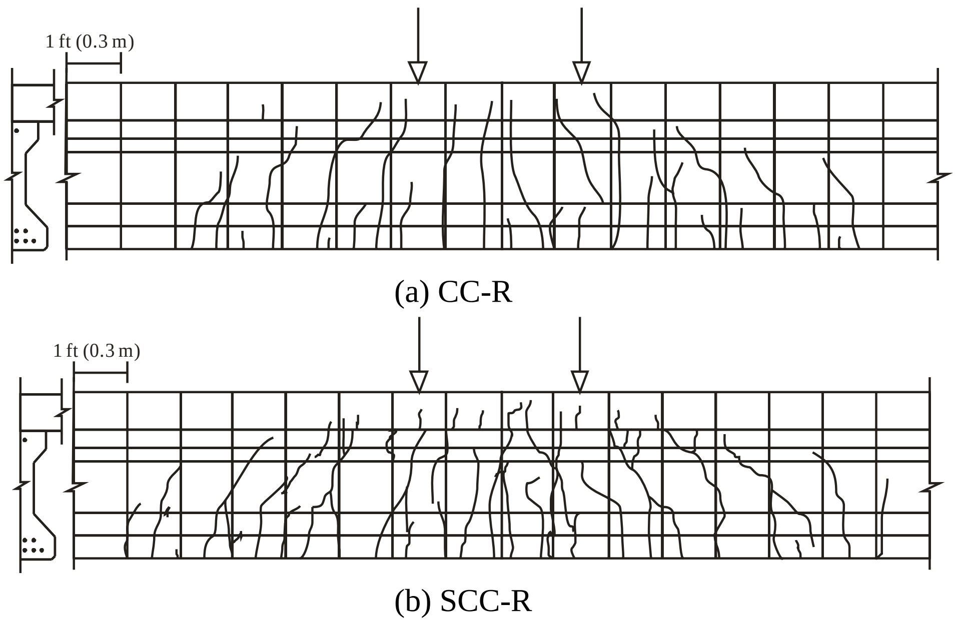

Fig. 16. Crack Diagram at Nominal Conditions

DEVELOPMENT LENGTH TESTS

After flexural test results at the midspan were compared, the development length tests were performed at each girder end. In this study, the point load (embedment length) was located 80 in. (2.0 m) from the girder end for the initial trial. If this length was found to be longer than the minimum development length, based on reaching nominal flexural conditions without a bond failure, a 70 in. (1.8 m) embedment length was used at the opposite end of the girder.

CC-R1 and CC-R2 Tests

The CC-R1 and CC-R2 tests were performed according to the test configurations shown in Figs. 6 and 7. At both ends, the girders were loaded to nominal flexural conditions and the failure mode was in flexure. The strain in the top fiber of the deck exceeded 3000 microstrain, indicating that the nominal flexural demand was achieved without bond failure. The flexural failure with an embedment length of 80 in. (2 m) indicates that the minimum development length is likely less than 80 in. (2.0 m) for the CC-R1 test. However, the same strain level was achieved for the CC-R2 test, indicating the minimum development length is likely less than 70 in. (1.8 m). Fig. 17 shows the moment-curvature of the girder for the development length tests for girder CC-R. Based on both tests, the minimum development length was found to be less than 70 in. (1.8 m).

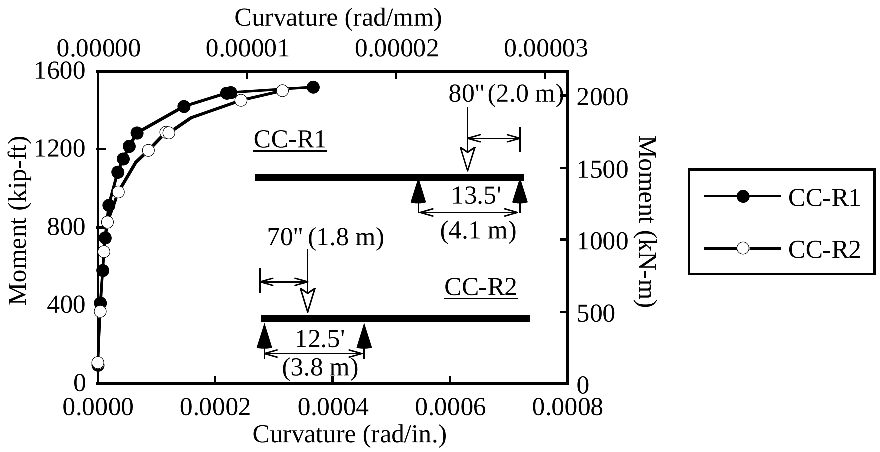

Fig. 17. Moment-Curvature of CC-R1 and CC-R2

SCC-R1 and SCC-R2 Tests

For the SCC-R1 test, the span length was 13.5 ft (4.1 m) with the same loading locations as the CC-R1 test. Fig. 18 shows the primary cracks for the test SCC-R1. Initially, there were diagonal shear cracks in the web, 3 ft (1 m) from the girder end. This cracking occurred at 250 kips (1110 kN). For this first test, a premature bond failure seemed to be caused by existing flexural cracks. As shown in Fig. 18, the flexural cracks that were present from the midspan flexural testing potentially shortened the free end of strands for the development length test. Thus, the 88 in. (2.2 m) length from the loading point to the inner support may have reduced the embedment length to approximately 76 in. (1.9 m). When the applied load reached 300 kips (1334 kN), extensive diagonal shear cracks on the web of the span adjacent to the inner support weakened this region. At about 380 kips (1690 kN), the span finally failed by bond splitting failure accompanied by shear cracks passing through the damaged region at the interior support.

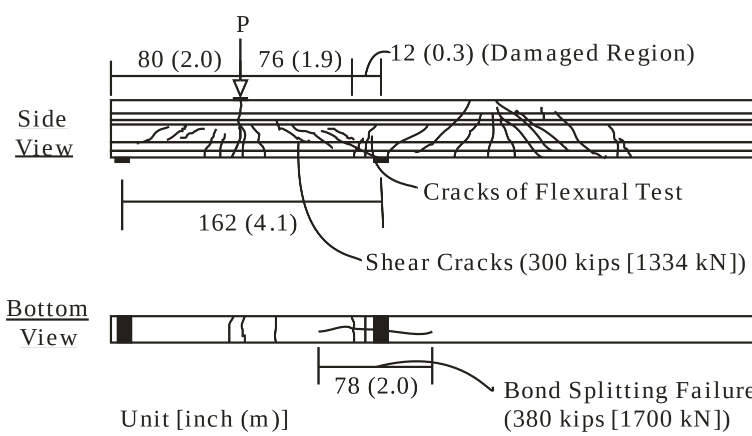

Fig. 18. Primary Cracks of SCC-R1

In addition to the presence of flexural cracks near the interior support, the self-weight of the overhanging portion of the girder induced negative moments on the inner support resulting in compression stresses at the bottom fiber near the support. Therefore, the shear and moment capacities were reduced near the interior support. This led to a modification in the test set-up where the overhead crane was used to support the girder weight at the free end and the interior support was moved further away from the cracked region caused by the flexural test, as shown in Fig. 8.

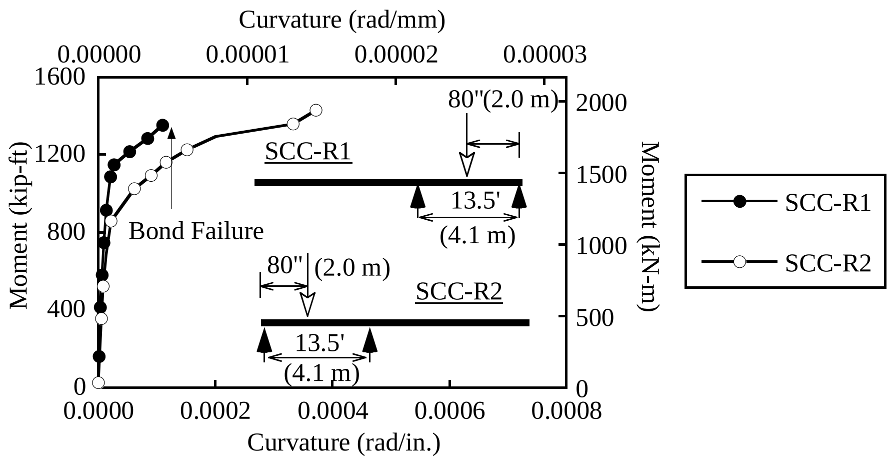

Fig. 19. Moment-Curvature of SCC-R1 and SCC-R2

Fig. 19 shows the moment-curvature plots for the SCC-R development length tests. The SCC-R1 results indicated that the girder resisted the applied load with brittle shear behavior rather than ductile flexural behavior. Therefore, the SCC-R1 had less curvature with respect to the same applied load for SCC-R2. The SCC-R2 test was loaded to nominal flexural conditions with an 80 in. (2.0 m) embedment length. This result indicates that the strain of the strands could reach the nominal state without bond failure and the development length is not greater than 80 in. (2.0 m).

Comparisons between Experimental Results and AASHTO LRFD

Bond failure did not occur in the development length tests, except for SCC-R1. After modifying the test set-up, the 80 in. (2 m) development length was sufficient and resulted in reaching the nominal flexural condition. When monitoring the slip of strands at the girder end, slip was less than 0.01 in. (0.25 mm), indicating no bond failure. It should be noted that although premature bond failure was observed in the SCC-R1 specimen near the interior support, there was no strand slip at the girder end, indicating no bond failure. In summary, the development length is likely shorter than 70 in. (1.8 m) for girders containing CC and SCC with similar configurations and material properties as those tested. However, due to limited test specimens, the development length for the SCC girder should be taken as 80 in. (2.0 m).

Eq.1 was used to compute the development length required by the AASHTO LRFD Specifications (2006). When the required development length was evaluated, the AASHTO LRFD equation for average strand stress at nominal flexural resistance, f_{ps}, and the measured effective prestress, f_{pe} , were used. The values of f_{ps} was calculated based on Article 5.7.3.1.1-1 of the AASHTO LRFD Specifications (2006) for each girder. The effective prestress, f_{pe} , values for each girder were obtained from the long-term measurements. Table 11 summarizes the development length test results and the computed l_d values. The 2006 AASHTO LRFD development length equation provided a conservative estimate of l_d for both the CC and SCC girders.

Table 11. Summary of Development Length Test Results

Test I.D.	l_d , in. (m)	Estimated l_d , in. (m)	2006 AASHTO l_d , in. (m)	Failure Mode
CC-R1	< 80 (2.0)	< 70 (1.8)	> 119 (3.0)	Flexural
CC-R2	< 70 (1.8)			Flexural
SCC-R1	Bond Failure	< 80 (2.0)	> 121 (3.1)	Shear/Bond
SCC-R2	< 80 (2.0)			Flexural

CONCLUSIONS

Based on conventional mechanical tests and full-scale girder testing, the following conclusions are drawn.

1. The SCC mixture had proper fresh characteristics with high workability without vibration. The SCC girder was fabricated in reduced time with less manpower and provided a smooth surface finish.
2. The strength development of the SCC mixture was excellent when compared to the CC mixture. The SCC compressive strength was about 30 percent higher than the CC compressive strength at 91 days.
3. The SCC girder had elastic and long-term prestress losses that are comparable to the CC girder. The 2006 AASHTO LRFD expressions overestimated the long-term prestress losses for both the SCC and CC girders at 140 days.
4. The SCC girder had shorter average measured transfer lengths when compared with the CC girder. The 2006 AASHTO LRFD Specifications provide a conservative estimate of the transfer lengths for both girders.
5. The measured development lengths for the SCC and CC girders are similar. The 2006 AASHTO LRFD Specifications provide a conservative estimate of the development lengths for both girders.
6. There was no evidence of bond failure or slip of strands during flexural testing.
7. The flexural behavior was comparable for the SCC and CC girders. Overall deflection histories were similar prior to destructive testing. Cracking moments are within 5 percent of each other. Although the SCC girder exhibited more flexural cracks when compared to the CC girder, the progress of the flexural cracks and maximum crack widths are similar. Moment-curvature responses and nominal moments are nearly identical.

ACKNOWLEDGMENTS

The authors acknowledge support and funding by the Texas Department of Transportation (TxDOT) through the Texas Transportation Institute (TTI) at Texas A&M University (TAMU). The valuable input of J. Tucker, J. Roche, J. Seiders, R. Browne, J. Moore, P. Almeida, P. Forsling (all of TxDOT) and H. Atahan (Post-Doctoral Research Associate at TTI) are appreciated. The authors also wish to thank P. Keating, M. Potter, S. Smith, and J. Perry of the Civil Engineering High Bay Structural and Materials Laboratory at TAMU and all of the students who assisted with the project. The authors also wish to thank Al Pinnelli at BASF Admixtures, Inc. for providing assistance and the admixtures. Plant testing and fabrication of the girders was done at the Texas Concrete Company, Victoria, Texas. The research team thanks B. Patton from Texas Concrete Company.

REFERENCES

1. ACI Committee 237. "Self-Consolidating Concrete." ACI 237R-07, American Concrete Institute, Farmington Hills, Michigan, 2007, 32.
2. Ghezal, A., and Khayat, K. H. "Optimizing Self-Consolidating Concrete with Limestone Filler by using Statistical Factorial Design Methods." *ACI Materials Journal*, V.99, No.3, 2002, pp. 264-272.
3. EFNARC "European Guidelines for Self-Compacting Concrete." 2005, www.efnarc.org.
4. Okamura, H., and Ozawa, K. "Self-Compactable High Performance Concrete in Japan." *International Workshop on High Performance Concrete*, 1994, pp. 31-44.
5. FHWA and NCBC. "Q&A: What is the Status on the Use of Self-Consolidating Concrete in Bridges?" HPC Bridge Views, the Federal Highway Administration and the National Concrete Bridge Council, Skokie, IL, 2005, pp. 1-4.
6. AASHTO LRFD "Bridge Design Specifications and Commentary." American Association of Highway and Transportation Officials (AASHTO), Washington, D.C., 2006.
7. TxDOT."Bridge Design Manual." Texas Department of Transportation, 2001.
8. ASTM C33. "Standard Specification for Concrete Aggregates." Annual Book of ASTM Standards, ASTM, 2007.
9. Atahan, H. N., Trejo, D., and Hueste, M. D. "Applicability of Standard Equations for Predicting Mechanical Properties of SCC." *Self-Consolidating Concrete for Precast Prestressed Applications*, Puerto Rico, 2007, pp. 17-31.
10. Koehler, E. P., and Fowler, D. W. "Development of Self-Consolidating Concrete for Prestressed Bridge Beams." *Self-Consolidating Concrete for Precast Prestressed Applications*, Puerto Rico, 2007, pp. 1-15.
11. Russell, B. W., and Burns, N. H. "Measured Transfer Lengths of 0.5 and 0.6 in. Strands in Pretensioned Concrete." *PCI Journal*, V.41, No.5, 1996, pp. 44-65.
12. Bentz, E. C. "Sectional Analysis of Reinforced Concrete Members." University of Toronto, 2000.